NEOPLASIA
www.neoplasia.com

Volume 18 Number 1 January 2016 pp. 49–59 49

Targeting of CCL2-CCR2-Glycosaminoglycan Axis Using a CCL2 Decoy Protein Attenuates Metastasis through Inhibition of Tumor Cell Seeding[1]

Marko Roblek[*,2], Elisabeth Strutzmann[†], Christina Zankl[†], Tiziana Adage[‡], Mathias Heikenwalder[§,¶], Aid Atlic[#], Roland Weis[#], Andreas Kungl[†,‡,] and Lubor Borsig[*]**

*Institute of Physiology, University of Zürich and Zürich Center for Integrative Human Physiology, CH-8057 Zurich, Switzerland; [†]KF-University Graz, Graz Austria; [‡]ProtAffin Biotechnologie AG, Graz Austria; [§]Institute of Virology, Technische Universität München/Helmholtz Zentrum Munich für Gesundheit und Umwelt, Munich, Germany; [¶]Division of Chronic Inflammation and Cancer, German Cancer Research Center (DKFZ), Heidelberg, Germany; [#]VTU Technology GmbH, Grambach, Austria; [**]Antagonis Biotherapeutics, Graz Austria

Abstract

The CCL2-CCR2 chemokine axis has an important role in cancer progression where it contributes to metastatic dissemination of several cancer types (e.g., colon, breast, prostate). Tumor cell–derived CCL2 was shown to promote the recruitment of $CCR2^{+}/Ly6C^{hi}$ monocytes and to induce vascular permeability of $CCR2^{+}$ endothelial cells in the lungs. Here we describe a novel decoy protein consisting of a CCL2 mutant protein fused to human serum albumin (dnCCL2-HSA chimera) with enhanced binding affinity to glycosaminoglycans that was tested *in vivo*. The monocyte-mediated tumor cell transendothelial migration was strongly reduced upon unfused dnCCL2 mutant treatment *in vitro*. dnCCL2-HSA chimera had an extended serum half-life and thus a prolonged exposure *in vivo* compared with the dnCCL2 mutant. dnCCL2-HSA chimera bound to the lung vasculature but caused minimal alterations in the leukocyte recruitment to the lungs. However, dnCCL2-HSA chimera treatment strongly reduced both lung vascular permeability and tumor cell seeding. Metastasis of MC-38GFP, 3LL, and LLC1 cells was significantly attenuated upon dnCCL2-HSA chimera treatment. Tumor cell seeding to the lungs resulted in enhanced expression of a proteoglycan syndecan-4 by endothelial cells that correlated with accumulation of the dnCCL2-HSA chimera in the vicinity of tumor cells. These findings demonstrate that the CCL2-based decoy protein effectively binds to the activated endothelium in lungs and blocks tumor cell extravasation through inhibition of vascular permeability.

Neoplasia (2016) 18, 49–59

Introduction

Inflammatory chemokines are implicated in several chronic inflammatory diseases including rheumatoid arthritis, inflammatory bowel disease, atherosclerosis, and multiple sclerosis. There is accumulating evidence that chemokines play crucial roles during the establishment of primary cancerous lesions as well as metastases, and they are generally associated with a progressed state of cancer and poor prognosis [1–3]. Among inflammatory chemokines, CCL2 has been implicated in several crucial steps during cancer formation and metastasis including promotion of angiogenesis [4], recruitment of myeloid-derived suppressor cells [5–7], regulation of invasiveness of cancer cells [8,9], and induction of

Address all correspondence to: Lubor Borsig, Institute of Physiology, University of Zurich, Winterthurerstrasse 190, CH-8057 Zurich, Switzerland.
E-mail: lborsig@access.uzh.ch

[1] This work was supported by a grant from EuroNanoMed2 project NANODIATER managed by the Swiss National Foundation #31NM30-136033 (L.B.) and ERC starting grant LiverCancerMechanism (M.H.).
[2] Cancer Biology PhD program Zurich.
Received 27 May 2015; Revised 4 November 2015; Accepted 8 November 2015

1476-5586
http://dx.doi.org/10.1016/j.neo.2015.11.013

prosurvival signaling in different cancer cells [7,10,11]. Furthermore, high levels of CCL2 in circulation were associated with poor outcome for breast, prostate, and colon cancer patients due to high incidence of metastasis (reviewed in [3]). Recent studies provided evidence that CCL2-CCR2 signaling represents a crucial axis for the formation of the metastatic microenvironment, which was largely dependent on recruitment of inflammatory monocytes in breast, colon, and lung cancer models [12–16]. Lately, CCL2-mediated endothelial activation in the lungs was shown to be required for efficient tumor cell extravasation [14].

For a full chemotactic function, chemokines need to bind to glycosaminoglycan (GAG) chains, which are part of proteoglycans located at the surface of endothelial cells in the vasculature. This enables the formation of a solid-phase chemokine gradient [17]. Although chemokines can function as monomers and without binding to GAGs *in vitro*, chemokines require GAG-binding and oligomer-formation capability for their functionality *in vivo* [18]. Chemokine binding to its receptors induces a potent signaling only when the processed N-terminal part of the chemokine is not modified [19]. In the case of CCL2 and CCL5, a single methionine extension of the N-terminus generates a potent receptor antagonist [17]. An anti-inflammatory CCL2 mutant with enhanced binding affinity to GAGs and containing a CCR2-antagonist mutation has been recently developed and tested in various inflammatory animal models [20,21].

This first generation of CCL2 decoy protein contained two amino acid mutations (S21K and Q23R), which were introduced to increase GAG-binding affinity, as well as Y13A and an N terminal methionine addition to block CCR2 activation. For the second generation of CCL2-based therapeutic mutant proteins, one additional basic amino acid was introduced into the chemokine sequence, S34K, to further enhance the GAG binding affinity. Because the protein consists of 77 amino acids, a rapid elimination from circulation was expected. For chronic therapeutic indications with parental application, however, we aimed to extend its serum half-life to prolong exposure. This was achieved by C-terminal fusion of the mentioned CCL2-based decoy protein to human serum albumin, which improved not only *in vivo* pharmacokinetic parameters but also the chemokine displacement pattern and the protein oligomerization behavior compared with the unfused decoy protein [22]. This novel fusion decoy protein with high therapeutic value (referred to as dnCCL2-HSA chimera) aims to target specific GAG structures in a similar way as antibodies target antigens. Here we present first *in vivo* data derived from experiments in which the CCL2-HSA chimeric protein was tested for its activity in a murine metastasis model.

Material and Methods

Cell Culture

Mouse colon carcinoma cell line MC-38 stably expressing GFP (MC-38GFP) was grown in Dulbecco's modified Eagle's medium with 10% fetal calf serum (FCS), and Lewis lung carcinoma cells (3LL) were grown in RPMI medium with 10% FCS [23,24].

dnCCL2 and dnCCL2-HSA Chimera Definition

The unfused CCL2 mutant (Met-CCL2 Y13A S21K Q23R S34K = dnCCL2) was produced in *Escherichia coli* and characterized as previously described [21]. The dnCCL2-based CCL2-HSA chimera was produced in *Pichia pastoris* and was purified by a two-step downstream process. The expression, purification, and characterization of this dnCCL2-HSA chimera are described in detail somewhere else [22]. In Figure 1, the schematic structure of the dnCCL2-HSA chimera is shown.

Surface Plasmon Resonance (SPR)

Binding of CCL2, dnCCL2, and dnCCL2-HSA chimera to unfractionated low–molecular weight heparin (Iduron, Manchester, UK) was investigated on a BiacoreX100 system (GE Healthcare) as described earlier [25]. Briefly, measurements were performed under a steady PBS flow containing 0.005% Tween. Biotinylated heparin was coupled on a C1 sensor chip, and each chemokine was measured at seven different concentrations. Contact times for all injections and dissociations were 120 seconds at 30 µl/min over both flow cells. Affinity constants were determined by a simple 1:1 equilibrium binding model where Req is plotted against the analyte concentration. Data were fitted using the steady-state formula that corresponds to the Langmuir adsorption equation provided by the Biacore Evaluation Software.

Migration Assay

The ability of dnCCL2-HSA chimera, dnCCL2, and CCL2 to induce the migration of freshly prepared human blood–derived monocytes was investigated using a 48-well Boyden chamber with a porous membrane (5-µm pore size; Neuroprobe, MD, USA). Human whole blood was obtained from healthy volunteers by venipuncture into heparinized tubes (Vacuette, GBO, Austria). Monocytes were isolated using Ficoll-Paque PLUS (GE Healthcare). The Buffy coat was aspirated and washed thrice with Hank's balanced salt solution, and cells were resuspended in Hank's balanced salt solution (2×10^6 cells/ml). Protein dilutions ranging from 20 to 2000 nM in PBS were placed in the lower chambers, and the chemotactic potential was

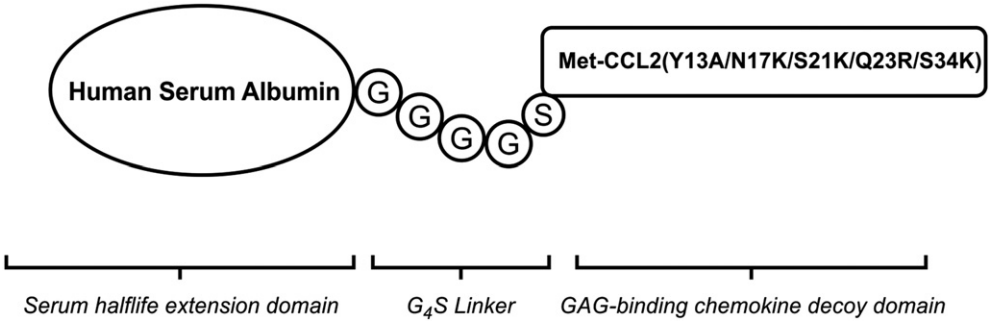

Figure 1. The schematic structure of the dnCCL2-HSA chimera. CCL2 mutant (Met-CCL2 Y13A S21K Q23R S34K) was fused through a Gly-linker to human serum albumin, expressed and purified as described in Material and Methods.

measured for each concentration 3 times. Freshly prepared monocytes (10^5 monocytes) were seeded in the upper chamber and incubated for 1 hour at 37°C. After the incubation, the insert was removed from the chamber, and cells attached on the lower side were fixed with methanol and stained with Hemacolor solutions (Merck, Germany). Cells were then counted at 40× magnification in 5 randomly selected microscopic fields per well.

Pharmacokinetics of dnCCL2 and dnCCL2-HSA Chimera in Mice

Animal care and handling procedures were performed in accordance with European guidelines, and all experiments were conducted under conditions previously approved by the local animal ethics committee in Graz. C57BL/6 male mice (Harlan, Italy), 6 to 8 weeks old, were intravenously injected with dnCCL2 (200 μg/kg body weight) or dnCCL2-HSA chimera (1600 μg/kg body weight, corresponding to 200 μg/kg dnCCL2 molar equivalent) in the lateral tail vein. At defined time points, blood was collected by heart puncture of deeply anesthetized mice (groups n = 3/time point) that were then euthanized. The serum concentration of dnCCL2 or dnCCL2-HSA chimera was analyzed using human MCAF ELISA kit (Hölzel, Germany). ELISA setup was performed according to the manufacturer's protocol and previously verified for cross-reactivity with both dnCCL2 and dnCCL2-HSA chimera. Data are reported as ng/ml of dnCCL2 equivalent, the active part of the molecule, to allow direct comparison of the pharmacokinetic profiles.

Mice

Animals were maintained under standard housing conditions, and experiments were performed according to the guidelines of the Swiss Animal Protection Law and approved by Veterinary Office of Kanton Zurich. C57BL/6 mice were purchased from Jackson Laboratory.

In Vitro Transmigration Assay

Primary pulmonary endothelial cells were isolated using a positive immunomagnetic selection as described previously [14]. Briefly, lungs were perfused with PBS and digested with 1 mg/ml of collagenase A (Roche, Basel, Switzerland) purified with anti-CD31 antibody (Life Technologies, Carlsbad, CA) coupled to anti-rat IgG MicroBeads (Miltenyi Biotec, Bergisch Gladbach, Germany). Primary lung microvascular endothelial cells (3×10^4) were seeded on gelatin coated 24-well Transwell inserts with 8-μm pores (BD, San Diego, CA) and allowed to grow to confluency (2 days). Tumor cells (2×10^4) were seeded into Transwell inserts with or without monocytes (1×10^5) in 3% FCS/RPMI in the upper chamber and 10% FCS/RPMI in the lower chamber. The transmigration lasted for 16 hours in the presence or absence of 10 μg/ml or 100 μg/ml of dnCCL2, 10 μg/ml of Maraviroc (R&D Systems, England), or 400 U/ml of Tinzaparin (Leo Pharmaceuticals, Denmark). The number of transmigrated cells (MC-38GFP) was counted on the bottom of the insert membrane with a Zeiss AxioVision microscope (n = 3-4).

Isolation of Bone Marrow Monocytes

Long bones from 6- to 8-week-old C57BL/6 mice were dissected, and the bone marrow was flushed with RPMI 1640 + 2% FCS medium. After red blood cell lysis (150 mM NH_4Cl, 10 mM $KHCO_3$, 0.1 mM EDTA), monocytes were purified with anti-CD115-biotin antibody (eBioscience, San Diego, CA) coupled to Streptavidin MicroBeads (Miltenyi Biotec). Monocytes ($CD115^+$) were used for the transmigration assay.

Analysis of Myeloid Cells from Blood and Lungs, and Cell Lines by Flow Cytometry

C57BL/6 mice were intravenously injected with 3×10^5 MC-38GFP cells. Mice treated with a dnCCL2-HSA chimera (800 μg) received 1 intravenous injection 10 minutes before tumor cell administration. After 12 hours, lungs were perfused with PBS and digested with collagenase A and collagenase D (each 2 mg/ml, Roche) for 1 hour. Cells were filtered through a 70-μm cell strainer (BD), and the single cell suspension was stained first with LIVE/DEAD Fixable Aqua Dead Cell Stain kit (Life Technologies) followed by antibody staining: anti–CD45-Pacific Blue (Biolegend, San Diego, CA), anti–CD11b-PE-CF594 (BD), anti–Ly6G-APC-Cy7 (BD), and anti–Ly6C-BV570 (BD). Data were acquired with an LSR II Fortessa machine (BD) and analyzed by FlowJo software (Tree star).

Blood samples (80 μl) were taken sublingually, diluted with 2 ml of 5 mM EDTA in PBS (EDTA/PBS), and centrifuged for 5 minutes at 500*g*. To lyse erythrocytes, cells were resuspended in 1 ml of PharmLyse (BD) and incubated for 15 minutes at room temperature. Cells were centrifuged for 5 minutes at 500*g*; resuspended in FACS buffer (10 mM EDTA, 2% FCS, in PBS); stained with CD45-APC-Cy7, CD11b-PE-Cy7, Ly6G-PerCP-Cy5.5, and Ly6C-FITC (all from BD); and then acquired with a FACSCanto (BD) machine. The results were analyzed by FlowJo software (Tree star).

Tumor cell lines MC-38GFP and LLC1, and the macrophage cell line RAW264.7 were detached from cell culture flasks by 2 mM EDTA/PBS for 10 minutes and stained with either anti–CCR2-PE (R&D Systems) or isotype-PE control (Biolegend). Data were acquired with a FACS Canto machine (BD) and analyzed by FlowJo software (Tree star).

Cell Sorting of Pulmonary Endothelial Cells

C57BL/6 mice were intravenously injected with 3×10^5 MC-38GFP cells. After 12 hours, lungs were perfused with PBS and digested with collagenase A and collagenase D (each 2 mg/ml, Roche) for 1 hour. Cells were filtered through a 70-μm cell strainer (BD), and the single cell suspension was stained with anti–CD45-Pacific Blue (Biolegend), anti–CD11b-APC-Cy7, anti–CD31-PE-Cy7, and anti–Ly6C-FITC (all BD). Endothelial cells ($CD31^+$) were sorted.

Immunohistochemistry (Frozen Sections)

Lungs of naive and tumor cell–injected mice were prepared for cryopreservation as previously described [23]. Lung sections (8 μm) were stained with anti-CD11b, anti-Ly6G (both from BD), and anti-F4/80 (AbD Serotec, Oxford, UK) followed by goat anti-rat AF568 (Life Technologies) antibodies. DAPI was used for nuclear staining. Pictures were taken with a Zeiss AxioVision microscope.

Histology and Immunohistochemistry

Lungs fixed in 4% paraformaldehyde were embedded in paraffin blocks. Lung sections (2 μm) were stained with hematoxylin/eosin or with antibodies anti-GFP (Fitzgerald Industries Int.) and anti-HSA (Sigma Aldrich, St. Louis, MO). Staining was performed on a NEXES immunohistochemistry robot (Ventana Instruments, Switzerland) using an IVIEW DAB Detection Kit (Ventana) or on a Bond MAX (Leica). Images were digitalized on Zeiss Mirax Midi Slide Scanner and analyzed with Panoramic Viewer (3DHISTECH).

Vascular Permeability Assay

C57BL/6 mice were intravenously injected with 3×10^5 MC-38GFP cells with or without prior dnCCL2-HSA chimera (800 μg intravenously) treatment. Twenty-four hours later, 2 mg of Evans blue (Sigma Aldrich)

was intravenously injected, and lungs were perfused with PBS 30 minutes later as described previously [14]. Lungs were dissected, photographed, and homogenized. Evans blue was extracted with formamide, and the amount was measured with a spectrophotometer (absorbance at 620 nm).

Experimental Metastasis

C57BL/6 mice were intravenously injected with 3×10^5 MC-38GFP or 1.5×10^5 3LL cells, respectively [14]. Mice were intravenously treated with indicated amounts of dnCCL2-HSA chimera 10 minutes before tumor cell injection and 24 hours post tumor cell injection. Mice were euthanized 28 days later, lungs were photographed, and the number of metastatic foci was determined.

Spontaneous Metastasis

Lewis lung carcinoma cells (LLC1, 300,000 cells) were subcutaneously injected into C57BL/6 mice. Mice were treated with intravenous injection of dnCCL2-HSA chimera (70 μmol = 800 μg) on day 11, on day 13, and at the time of tumor removal (day 15). Mice were terminated 2 weeks after surgical removal of the subcutaneous tumor (total day 29). The lungs were perfused with PBS, and the number of metastatic foci was counted.

RNA Isolation and Reverse Transcription

Thirty milligrams of lung tissue was transferred to a mortar, homogenized in liquid nitrogen, and lysed, and total RNA was extracted using GenElute Total Mammalian RNA Miniprep Kit (Sigma Aldrich) according to the manufacturer's protocol. Purity and quantity of the eluted RNA were determined by measuring the absorption at 260 and 280 nm. Two micrograms of total RNA was transcribed into cDNA using "High Capacity cDNA Reverse Transcription Kit" (Applied Biosystems).

Quantitative Real-Time Polymerase Chain Reaction (qPCR)

The mRNA expression of the target genes was analyzed with a qPCR assay using the SYBR Green I chemistry in an AB 7300 Real-Time PCR System Instrument (Applied Biosystems). Samples were heated to 95°C for 10 minutes, followed by 40 cycles of 95°C for 15 seconds, 55°C for 30 seconds, and 72°C for 1 minute. Quantitative real-time PCR was carried out with a final sample volume of 20 μl, containing 10 μl of Kapa SYBR Fast qPCR MasterMix for ABI Prism (Peqlab), 5 μl of the primer mix (2 μM each, forward and reverse; Invitrogen, Life Technologies), 0.5 μl of template cDNA, and 4.5 μl of nuclease-free water (Ambion, Life Technologies). The housekeeping enzyme glyceraldehyde 3-phosphate dehydrogenase (GAPDH) was used as an endogenous control. Group size was $n = 4$ to 5. Oligonucleotide sequences used for amplification are shown in Table 1. Expression levels are shown relative to GAPDH or to isolated cells from naive mice.

Table 1. Mouse Primer Sets Used in Real-Time PCR Analysis

Protein Name	Primer Set	Gene
Syndecan-1	5′AGGATGGAACTGCCAATCAG 3′ATCCGGTACAGCATGAAAGC	SDC1
Syndecan-2	5′TCTGAGGCAGAAGAGAAGCTG 3′AGGATGAGGAAAATGGCAAA	SDC2
Syndecan-3	5′ATACTGGAGCGGAAGGAGGT 3′TTTCTGGTACGTGACGCTTG	SDC3
Syndecan-4	5′AACCACATCCCTGAGAATGC 3′AGGAAAACGGCAAAGAGGAT	SDC4
Glypican-1	5′GGCCATCATGAAGTTGGTCT 3′ACACCGCCAATGACACTCTC	GPC1
Glypican-2	5′TGAATGAGCAGCTCCACAAC 3′TCGTCTGCATACTGCTGTCC	GPC2
Glypican-3	5′TGTGCCCAAGGGTAAAGTTC 3′AGGTGGTGATCTCGTTGTCC	GPC3
Glypican-4	5′CGTTTGCAATGATGAGAGGA 3′GCCATGATCTGACGAAGGAT	GPC4
Glypican-5	5′AGATGGCTGTGGAGGATCAG 3′GACTCAGTTCCTGACGCACA	GPC5
Glypican-6	5′GTGCCACGGAAACTGAAGAT 3′GGCCGAAGATTCCTCTTCTC	GPC6
E-selectin	5′CGCCAGAACAACAATTCCAC 3′ ACTGGAGGCATTGTAGTACC	SELE
GAPDH	5′AGCTTGTCATCAACGGGAAG 3′CCTTCCACAATGCCAAAGTT	GAPDH

Statistics

Statistical analysis was performed with the GraphPad Prism software (version 5.0). All data are presented as mean ± SEM and were analyzed by analysis of variance with the *post hoc* Bonferroni multiple comparison test, unless specified differently.

Results

Pharmacological Blocking of CCL2 Inhibits Tumor Cell Transmigration In Vitro

A signaling-deficient CCL2 chemokine decoy protein with enhanced GAG-binding affinity was previously shown to inhibit recruitment of inflammatory leukocytes *in vivo* [21]. To further improve the therapeutic potential of CCL2-based decoys, the chemokine has been additionally engineered and fused to human serum albumin (HSA) to extend the serum half-life and to optimize the GAG-binding protein displacement profile with the aim to avoid off-target effects [22]. First, we measured the affinity of the unfused CCL2 mutant (designated as dnCCL2) and the HSA-coupled dnCCL2 (further designated as dnCCL2-HSA chimera; Figure 1) toward heparin using SPR measurement. We observed a significantly enhanced affinity to heparin of both dnCCL2 and dnCCL2-HSA chimera compared with wild-type CCL2 (Figure 2*A*). Next, we tested the chemotactic activity of dnCCL2 and dnCCL2-HSA chimera and compared it with the wild-type CCL2 control. Both mutant proteins did not induce monocyte migration when tested in the range of 20 to 2000 nM, which was in contrast to a strong chemotactic activity induced by the wild-type CCL2 (Figure 2*B*). Finally, dnCCL2 was tested for its activity in a murine model, which we selected for the analysis of CCL2-CCR2 axis in cancer progression. For this purpose, we selected MC-38GFP cells, which were shown to produce CCL2 and metastasize in a CCL2-dependent manner [14,15] and do not express CCR2 (Figure 2*D*). The capacity of dnCCL2 to affect monocyte-facilitated tumor cell (MC-38GFP) transmigration through a monolayer of pulmonary microvascular endothelial cells was tested using the Boyden chamber assay (Figure 2*C*). Although monocytes clearly potentiated endothelial transmigration of tumor cells [13,14], the presence of dnCCL2 at concentrations of 10 or 100 μg/ml significantly and dose-dependently attenuated this process. In contrast, there was no effect on tumor cell transmigration in the presence of a CCR5 inhibitor (Maraviroc) or of a low–molecular weight heparin, Tinzaparin. Heparin was tested for its potential to bind CCL2 and thereby interfere with endothelial transmigration. These data indicate that the GAG-mediated CCL2-CCR2 chemokine axis is critical for an efficient tumor cell transendothelial migration and more importantly that dnCCL2 is biologically active also in a murine cell–based system.

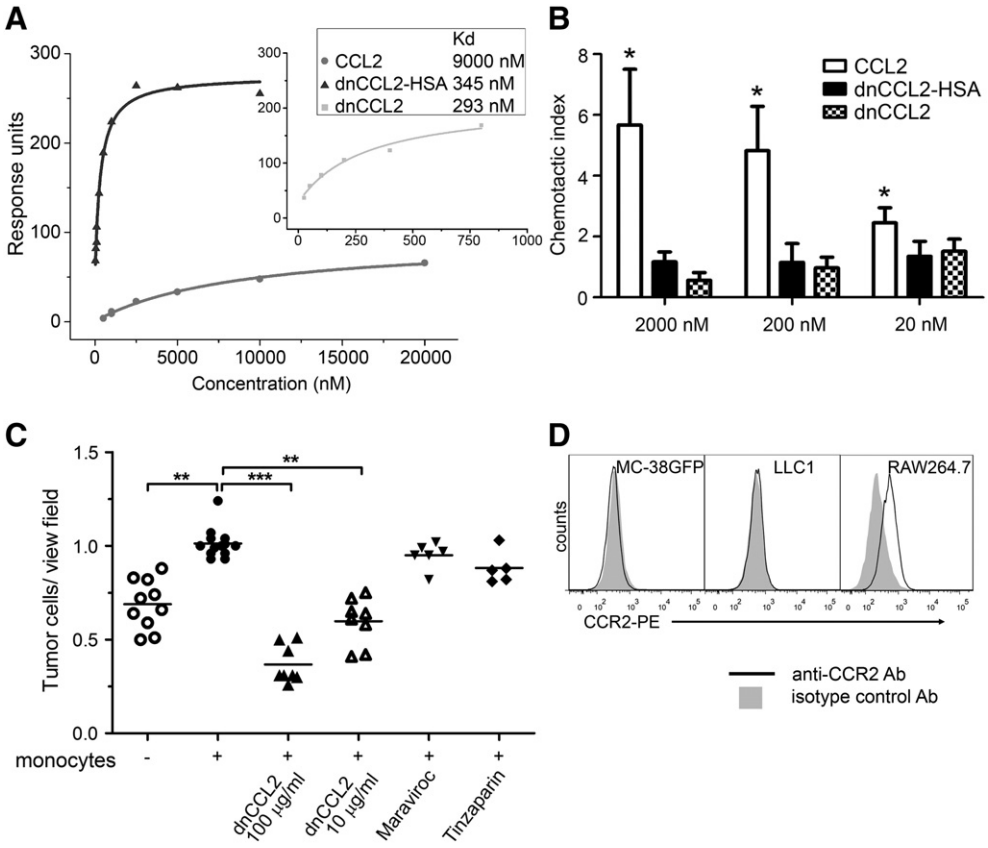

Figure 2. CCL2 decoy efficiently binds to glycosaminoglycans, blocks chemotaxis of monocytes, and inhibits transmigration of tumor cells across primary pulmonary endothelial cells. (A) Affinity of CCL2, dnCCL2, and dnCCL2-HSA chimera to heparin determined by SPR method. (B) Chemotactic activity of CCL2, dnCCL2, and dnCCL2-HSA chimera on human monocytes using Boyden chamber assay. The chemotactic index represents the mean cell number of migrated cells divided by the mean cell number of the cells migrated without stimuli. *$P < .05$. (C) Transendothelial migration of tumor cells through endothelial monolayers. MC-38GFP tumor cells were co-cultured with monocytes or without (control) on monolayers of endothelial cells for 16 hours. Inhibitors dnCCL2, 100 μg/ml and 10 μg/ml (CCR2); Maraviroc, 10 μg/ml (CCR5); and Tinzaparin, 400 U/ml (low–molecular weight heparin) were added to the co-culture. Transmigrated tumor cells were counted per view field and are presented in relative values. **$P < .01$; ***$P < .001$. (D) Expression of CCR2 on MC-38GFP and LLC1 cells. Macrophage cell line (RAW267.4) was used as a positive control.

dnCCL2 Exposure In Vivo Was Enhanced upon Conjugation to Human Serum Albumin

Before assessing the biological potentials of dnCCL2-HSA chimera *in vivo*, we assessed its pharmacokinetic profile in comparison to dnCCL2 upon intravenous injection of equimolar quantities (Figure 3). Following intravenous dosing of both dnCCL2-HSA chimera and dnCCL2, the mean serum profile showed concentration levels declining with an apparent biphasic distribution and elimination curves. The pharmacokinetic profiles were markedly different, with the former showing detectable levels up to 72 hours from administration, whereas, for the latter, no concentrations were detectable after 18 hours. The initial distribution phase for dnCCL2-HSA chimera showed a rapid decrease in concentrations followed by a slow log-linear elimination phase lasting from 4 hours up to 72 hours. Elimination was nearly complete at the final time point assessed, with the plasma concentration versus time curve (area under curve = $AUC_{0\text{-last}}$; 1761.3 h×ng/ml) being similar to the AUC extrapolated to infinity (1797.7 h×ng/ml) A long mean residence time of 12.2 hours was observed. The elimination phase (calculated from 4 hours onward) gave an apparent terminal half-life of 16.8 hours. Clearance value was low, namely, about 0.111 l/h per kilogram. In comparison, following dnCCL2 treatment, the initial distribution phase showed an even faster decrease in concentrations followed by a log-linear elimination phase lasting from 4 hours up to 18 hours only. Elimination was complete at 18 hours, with the $AUC_{0\text{-last}}$, (44.7 h×ng/ml) and the AUC to infinity (44.8 h×ng/ml) showing equal values. The mean residence time was exceptionally low, namely, 1.0 hour. The elimination phase, evaluated in the 4- to 18-hour interval, showed an apparent terminal half-life of 2.8 hours. Clearance value (4.461 l/h per kilogram) was very high. Taken together, the exposure following *dnCCL2-HSA chimera* intravenous administration was about 40 times higher than that observed after treatment with dnCCL2.

dnCCL2-HSA Chimera Reduces Tumor Cell–Induced Vascular Permeability and Tumor Cell Seeding to the Lungs

Initial recruitment of $Ly6C^{hi}$ cells was previously shown to promote tumor cell extravasation and thereby metastasis [13,14]. First, we tested whether dnCCL2-HSA chimera affects the number of circulating monocytes. We treated mice twice with 800 µg of dnCCL2-HSA chimera (corresponding to 100 µg of dnCCL2 equivalent) and quantified the number of myeloid cells in the blood (Figure 4*A*). We observed comparable numbers of $Ly6C^{hi}$ cells in both naive controls and dnCCL2-HSA chimera-treated mice. To determine whether dnCCL2-HSA chimera can inhibit the recruitment of monocytes *in vivo*, we analyzed infiltrating leukocytes to the lung 12 and 24 hours

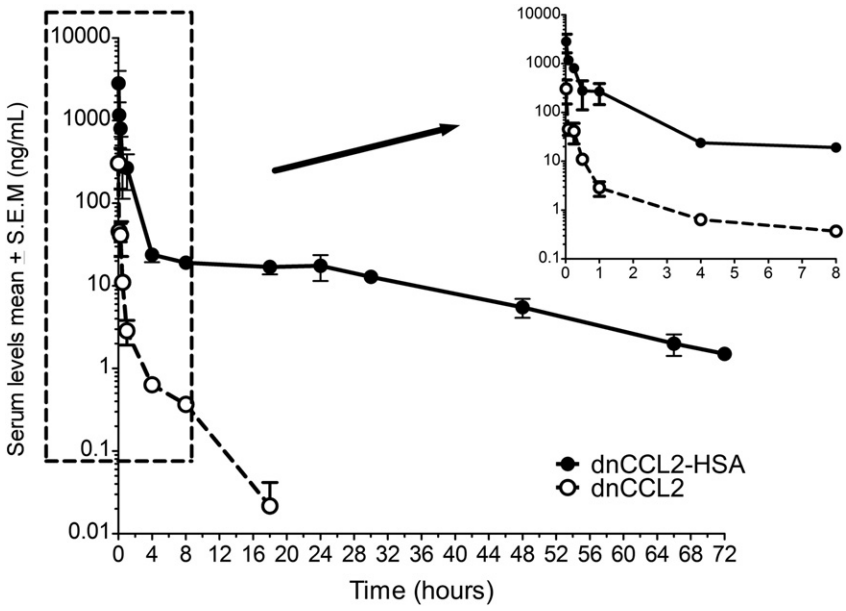

Figure 3. Pharmacokinetic profile of dnCCL2 and dnCCL2-HSA chimera *in vivo*. Mice were intravenously injected with dnCCL2 (200 μg/kg) and dnCCL2-HSA chimera (200 μg/kg dnCCL2 equivalent), and the serum levels of each protein were determined at different time points. $n = 3$. Data are reported as ng/ml of dnCCL2 equivalent, the active part of the molecule, to allow direct comparison of the pharmacokinetic profiles.

after intravenous injections of MC-38GFP cells by flow cytometry. Surprisingly, dnCCL2-HSA chimera treatment did not alter the recruitment of myeloid cells, including Ly6C^{hi} cells, to the lung of tumor cell–injected mice compared with controls (Figure 4*B*). We observed a similar increase in myeloid cells (CD11b$^+$ cells) after 12 hours, which was diminished after 24 hours (not shown), in the lungs of dnCCL2-HSA chimera–treated and control mice. To further test whether dnCCL2-HSA chimera affects the leukocyte recruitment to the arrested tumor cells in the lungs, we analyzed lung sections for tumor cell-leukocyte association 12 and 24 hours post tumor cell injection using immunohistochemistry. We observed an association of CD11b$^+$ cells with tumor cells that was reduced upon dnCCL2-HSA chimera treatment at 12 hours (Figure 4*C*). However, this reduction was not detected at 24 hours. We found an initially higher association of Ly6G$^+$ cells with tumor cells, which decreased over time independent of a treatment (Figure 4*C*). On the contrary, we observed equal association of F4/80$^+$ cells with tumor cells independent of time and treatment.

Next, we evaluated whether dnCCL2-HSA chimera treatment affects lung vascular permeability, which was shown to be dependent on tumor-derived CCL2 and endothelial CCR2 expression [14]. Mice treated with dnCCL2-HSA chimera showed reduced vascular leakiness compared with untreated mice as determined by Evans blue assay 24 hours post tumor cell injection (Figure 4*D*). To determine whether reduced vascular permeability in the presence of dnCCL2-HSA chimera affects tumor cell survival in the lungs and their extravasation, we analyzed lungs of mice intravenously injected with MC-38GFP cells after 6, 12, 24, and 48 hours (Figure 4*E*). Indeed, dnCCL2-HSA chimera treatment in mice significantly reduced the number of living tumor cells in the lungs at 24 hours when compared with control (untreated) lungs, and it remained reduced also after 2 days. These findings indicate that temporal inhibition of the CCL2-CCR2 axis by dnCCL2-HSA chimera treatment diminishes the ability of tumor cells to leave the vasculature.

dnCCL2-HSA Chimera Treatment Reduces Pulmonary Metastasis

To test the hypothesis as to whether the CCL2 decoy protein inhibits metastatic formation in the lungs, we used experimental metastasis model using MC-38GFP cells. We treated mice intravenously with the dnCCL2 or the dnCCL2-HSA chimera 10 minutes before tumor cell injection and 24 hours post tumor cell injection. Significant reduction of lung metastasis after 28 days was observed in mice treated with the dnCCL2-HSA chimera with two different doses: 17.5 μmol = 200 μg and 70 μmol = 800 μg, respectively (Figure 5, *A* and *B*). However, equimolar concentration of dnCCL2 (70 μmol = 100 μg) did not have any effect on metastasis, likely because of its fast elimination. Similarly, mice treated with HSA alone did not have reduced number of metastasis (Figure 5, *A* and *B*). Thus, we concluded that the prolonged serum half-life of the dnCCL2-HSA chimera is needed for the antimetastatic activity. dnCCL2-HSA chimera treatment of mice before injection of Lewis lung carcinoma cells (3LL) also attenuated metastasis (Figure 5*C*), indicating that this activity is tumor cell type independent. Finally, we tested the capacity of dnCCL2-HSA to inhibit spontaneous metastasis to the lungs of Lewis lung carcinoma cells (LLC1) upon subcutaneous injection. Indeed, three intravenous injections of dnCCL2-HSA, covering approximately 6 days during the time when tumor cell might be in circulation, attenuated metastasis (Figure 5*D*). These data confirmed that GAG-mediated CCL2-CCR2 axis promotes metastatic initiation, and a specific inhibition of CCL2 accumulation at the site of tumor cell extravasation can inhibit this process.

Metastasizing MC-38GFP Cells Induce Syndecan-4 (SDC4) Expression in the Lungs

Chemokine binding to GAGs on the endothelial surface enables formation of an intravascular chemokine gradient [17,18]. To investigate the mechanism of the dnCCL2-HSA chimera activity in the metastatic model, we first analyzed the expression of proteoglycans in the lungs 12 and 24 hours after injection of MC-38GFP cells. We observed no significant changes in mRNA expression of the different

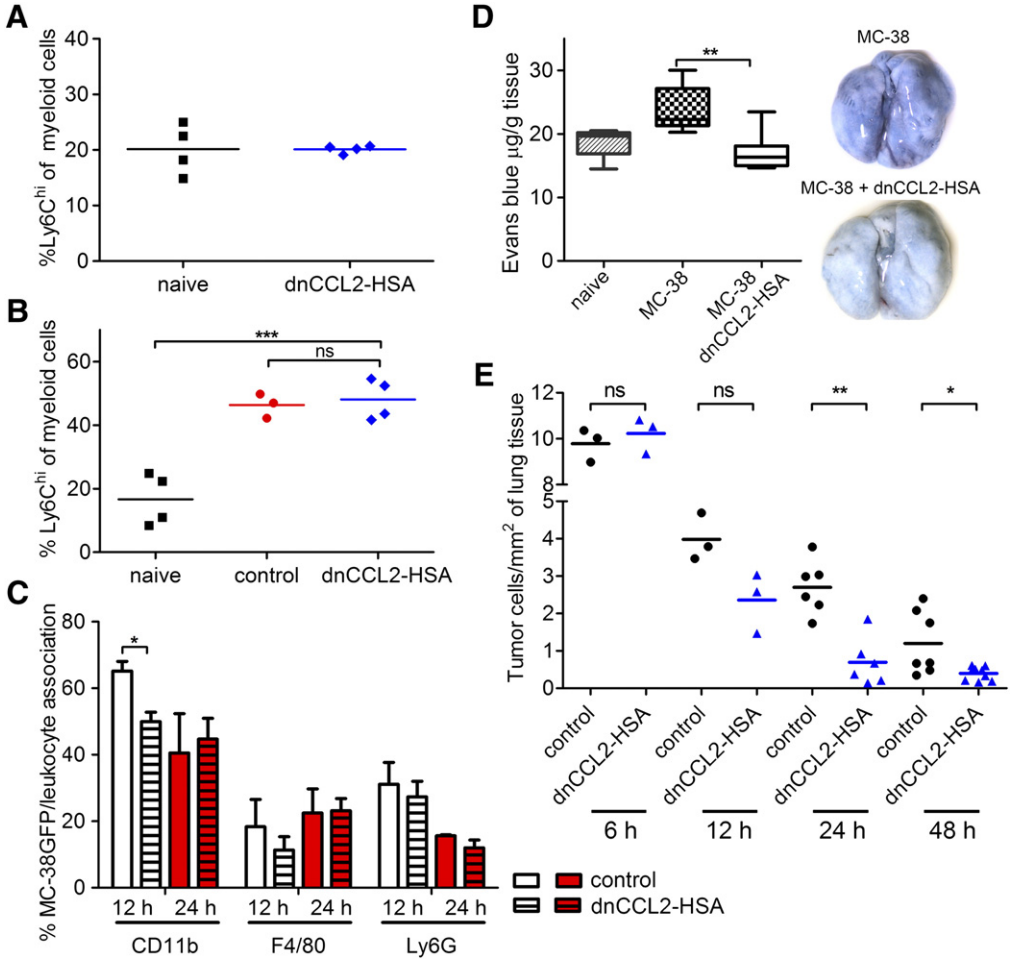

Figure 4. Lung analysis of mice intravenously injected with MC-38GFP cells with or without dnCCL2-HSA chimera treatment. (A) Flow cytometry analysis of myeloid cells in circulation after two intravenous injections (0 hour and 24 hours) with dnCCL2-HSA chimera (800 μg) analyzed 20 hours after the last treatment. ns = not significant (B) Flow cytometry analysis of myeloid cells in the lungs of MC-38GFP–injected mice treated with dnCCL2-HSA chimera or controls (untreated) after 12 hours compared with naive lungs (no tumor cell injection). (C) Histological analysis of tumor cell-leukocyte association from MC-38GFP–injected mice. Serial sections were evaluated for colocalization of $CD11b^+$, $Ly6G^+$ and $F4/80^+$ cells with tumor cells 12 and 24 hours after tumor cell injection. $n = 3$. Student's t test $^*P < .05$. (D) Vascular permeability determination. Evans blue extracted from lungs of mice injected with MC-38 cells 24 hours earlier and either treated or untreated with dnCCL2-HSA was normalized to the lung weight ($n = 6$). Mice without tumor cell injection were used as controls (naive). Representative macroscopic images are shown. Student's t test $^{**}P < .01$. (E) Tumor cell seeding in the lungs of mice 6, 12, 24, and 48 hours after intravenous injection of MC-38GFP cells evaluated by immunohistochemistry. dnCCL2-HSA chimera was injected at the time of tumor cell injection only. Mice without dnCCL2-HSA chimera injection (control) were used as controls.

syndecans and glypicans, with the exception of SDC4 (Figure 6*A*). SDC4 expression was significantly increased 12 hours post tumor cell injection. To confirm that the increase of SDC4 expression corresponded to endothelial cells, we sorted pulmonary endothelial cells from naive and from MC-38GFP–injected mice 12 hours postinjection. A two-fold increase in SDC4 expression was detected in pulmonary endothelial cells isolated from tumor-injected mice (Figure 6*B*). Tumor cell arrest in the lung vasculature was shown to lead to local endothelial activation [26]. To test whether SDC4 expression correlates with endothelial activation, we analyzed E-selectin expression. We observed a five-fold increase in E-selectin expression, which confirms the activation status of the endothelial cells. These data showed that tumor cells induce endothelial activation, which correlates with an enhanced expression of SDC4.

Enhanced accumulation of CCL2 in the lungs during the metastatic initiation has been observed [23]. To identify the potential of the dnCCL2-HSA chimera binding to GAGs, MC-38GFP–injected mice were either treated with 800 µg of dnCCL2-HSA chimeric protein or left untreated (control), and lungs were removed for analysis 12 and 24 hours post tumor cell injection. dnCCL2-HSA chimera was detected using anti-HSA antibodies. We observed dnCCL2-HSA chimera staining throughout the lung vasculature, with an enhanced presence detected in the proximity of MC-38GFP cells at 24 hours (Figure 6*E*). Treatment with HSA in MC-38GFP–injected mice resulted only in background staining (MC-38GFP/HSA). Similarly, mice injected only with MC-38GFP cells (control) or with HSA but without tumor cells (HSA) showed no staining. These data indicate that tumor cell–induced expression of SDC4 in the lungs correlates with dnCCL2-HSA chimera localization in the lung vasculature in the proximity of tumor cells.

Discussion

Chemokines are mediators of directed cell migration, such as leukocyte recruitment during inflammation, as well as cell activators of several other important cellular pathways (e.g., Jak or Stat signaling). CCL2 has been

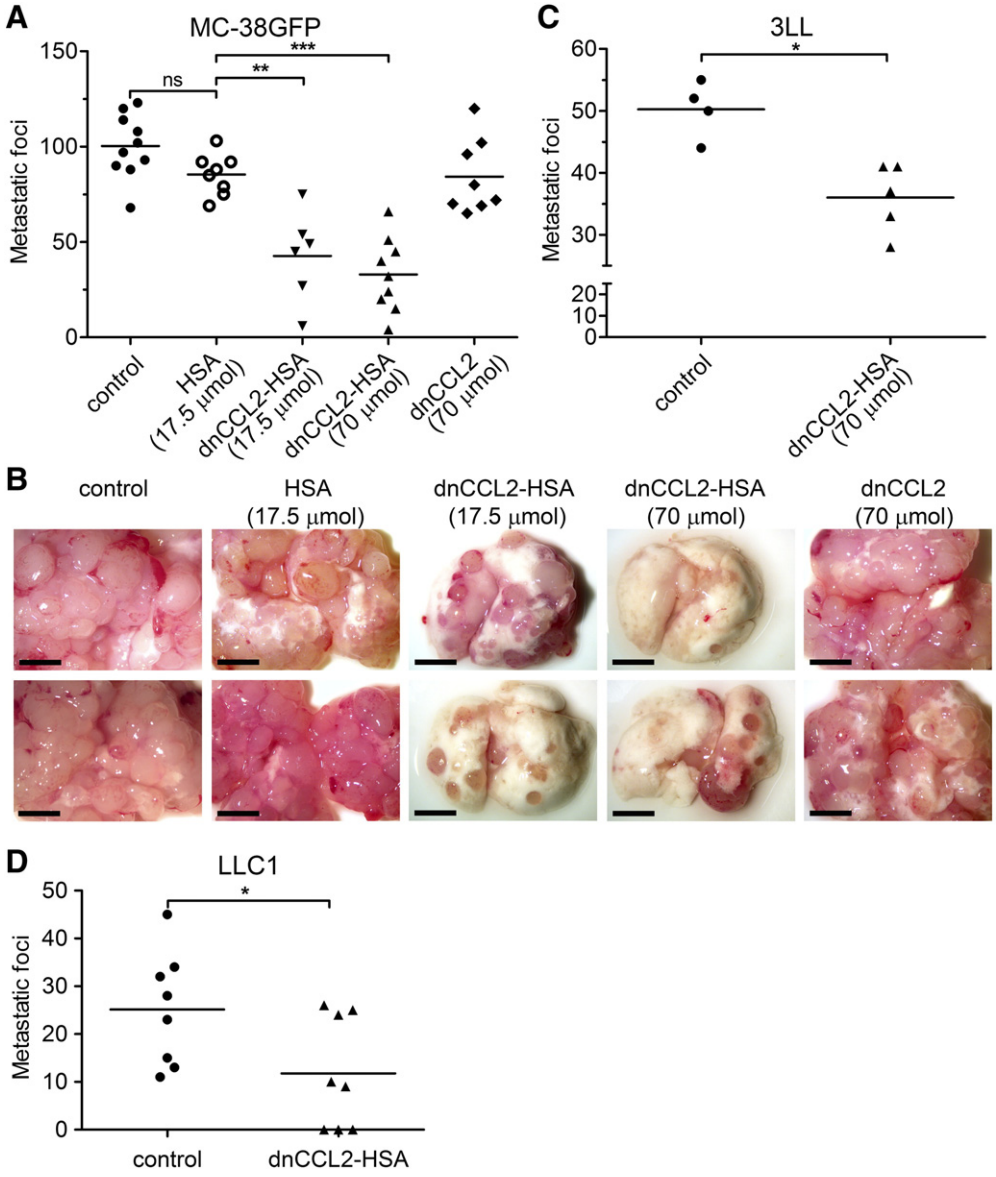

Figure 5. dnCCL2-HSA chimera reduces experimental metastasis. (A) Mice were intravenously injected with dnCCL2-HSA chimera (17.5 μmol = 200 μg or 70 μmol = 800 μg), HSA (17.5 μmol = 200 μg), or dnCCL2 (70 μmol = 200 μg) 10 minutes before and 24 hours after MC-38GFP cell application. Metastatic foci were quantified after 28 days. $^{**}P < .01$; $^{***}P < .001$. (B) Representative macroscopic images of perfused lungs from control and dnCCL2-HSA chimera–treated mice. (C) Mice were intravenously injected with dnCCL2-HSA chimera (70 μmol = 800 μg) 10 minutes before and 24 hours after 3LL cell application. Metastatic foci were quantified after 12 days. (D) Mice were subcutaneously injected with LLC1 cells and treated with intravenous injection of dnCCL2-HSA chimera (70 μmol) at days 11, 13, and 15. Lung metastasis was determined at day 30. Mann-Whitney test $^{*}P < .05$.

identified as a major cancer-associated chemokine, which promotes cancer progression through modulating both tumor cell metastatic behavior and the metastatic microenvironment [7,10,12–14]. CCL2-mediated recruitment of CCR2^{+} inflammatory monocytes (Ly6C^{hi}) facilitates tumor cell extravasation and metastasis. Recently, stromal CCR2 expression has been identified to also promote this process [12,14]. Specifically, activation of CCR2^{+} endothelial cells in the lungs is required for induction of vascular permeability and efficient tumor cell extravasation [14]. In another study, CCL2-mediated activation of brain endothelial cells resulted in decreased barrier function and increased vascular permeability [27]. Endothelial CCR2 expression in the brain is critical for transendothelial migration of macrophages that was absent in CCR2$^{-/-}$ brain microvascular endothelial cells upon CCL2 stimulation [28]. These studies showed that CCL2 triggering of endothelial CCR2 increases endothelial and vascular permeability and contributes to efficient leukocyte extravasation.

It is well established that CCR2 is required for inflammatory monocytes to leave the bone marrow after an inflammatory stimulus but appears to be dispensable for inflammatory monocytes to be recruited to sites of infection [29]. This observation is further supported by Soehnlein et al., who showed that the recruitment of Gr1^{hi} monocytes to atherosclerotic vessels is dependent on CCR1 and/or CCR5 axis but is dispensable of CCR2 [30]. Similarly, the chemotactic response of monocytes toward synovial fluid from rheumatoid arthritis patients showed that neither anti-CCR2 nor anti-CCR5 antibodies inhibited the recruitment, but CCR1-mediated recruitment was shown to be essential [31]. Because

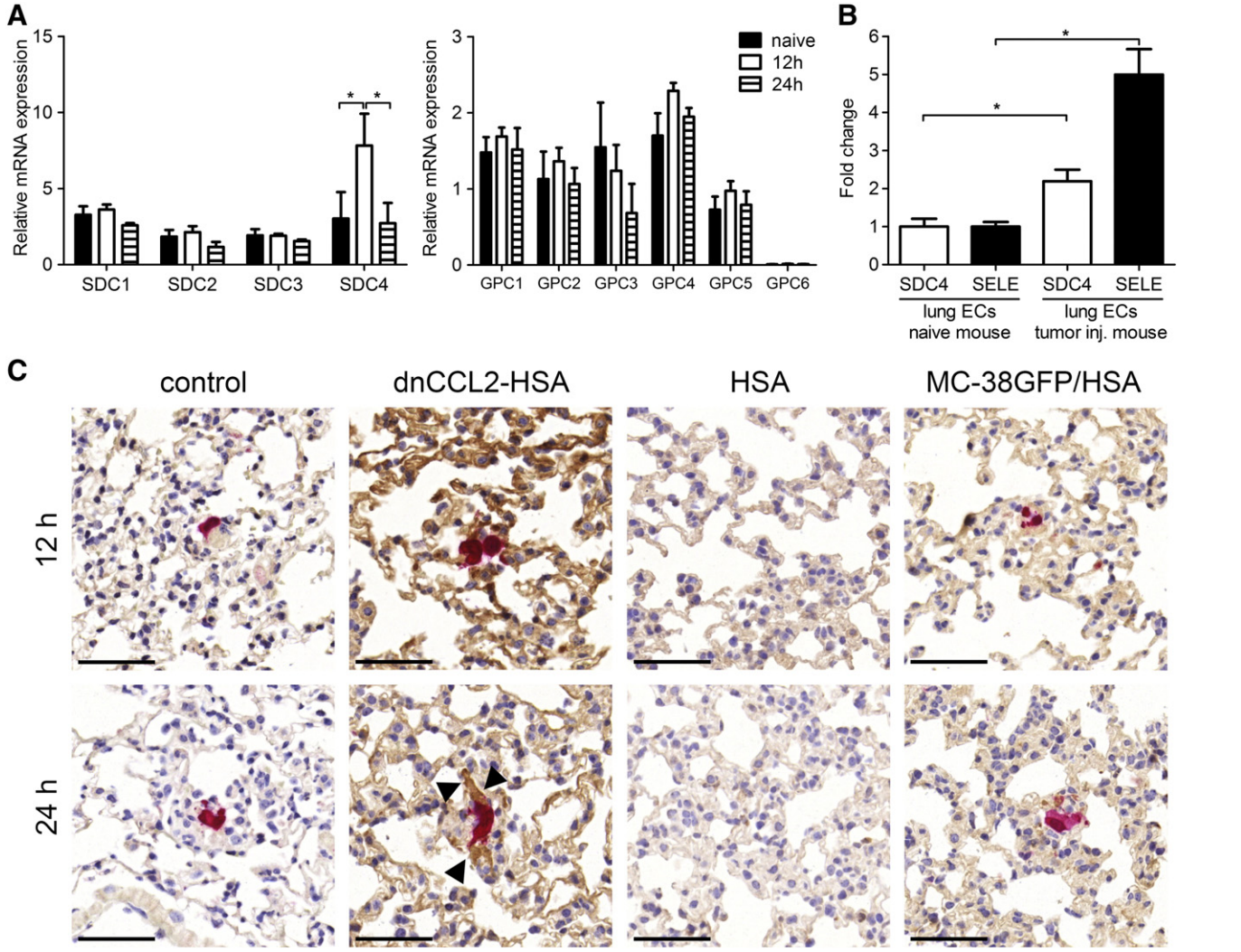

Figure 6. Increased SDC4 expression in lungs of tumor cell–injected mice correlates with the enhanced presence of dnCCL2-HSA chimera. (A) Proteoglycan expression in the lungs of mice 12 and 24 hours after MC-38GFP injection compared with naive mice. Relative mRNA expression levels of syndecans 1, 2, 3, and 4 and glypicans 1, 2, 3, 4, 5, and 6 normalized to GAPDH expression are shown. $n \geq 3$, $^*P < .05$. (B) Relative mRNA expression of SDC4 and E-selectin (SELE) in endothelial cells purified from lungs of naive and MC-38GFP–injected mice after 12 hours, respectively. Fold increase was normalized to naive endothelial cells. $^*P < .05$. (C) dnCCL2-HSA chimera staining (brown) of lungs from MC-38GFP (red)–injected mice after 12 and 24 hours using HSA antibody. Lungs of mice injected only with MC-38GFP (control), with dnCCL2-HSA chimera and MC-38GFP cells (dnCCL2-HSA chimera), with HSA only (HSA), and with HSA and MC-38GFP (MC-38GFP/HSA). Black arrowheads indicate the specific dnCCL2-HSA chimera staining around a tumor cell. Bar = 50 μm.

there are a number of chemokines potentially involved in monocyte recruitment to both the inflammatory sites and the metastatic microenvironment, further studies are required for identification of specific roles of chemokines during both inflammation and metastasis.

During cancer progression, CCL2 initiates endothelial activation and contributes to the recruitment of inflammatory monocytes to metastatic sites [12–16]. The use of a CCL2-neutralizing antibody reduced metastasis of breast cancer cells to the bone and the lungs [12,13]. The reduced recruitment of monocytes to the lung vasculature resulted in attenuated tumor cell extravasation. In a prostate cancer model, the use of neutralizing CCL2 antibody also resulted in attenuation of metastasis [32]. In addition, targeting of CCR2 with a small molecular inhibitor caused a reduction of primary tumor growth and liver metastasis of pancreatic adenocarcinoma cells [33]. The use of CCR2 inhibitor treatment reduced the number of inflammatory monocytes in the liver. However, the anti-CCL2 mAb Carlumab (CNTO888) showed no activity in patients with solid tumors due to transient reduction of CCL2 levels followed by a significant increase [34]. In the present study, we have not detected a reduced infiltration of inflammatory monocytes ($Ly6C^{hi}$) to the lungs 12 hours after intravenous tumor cell injection in dnCCL2-HSA chimera–treated compared with control mice. We observed reduced association of $CD11b^+$ cells with tumor cells 12 hours postinjection. In contrast, we showed evidence for reduced vascular permeability upon dnCCL2-HSA chimera treatment and reduced metastasis. Finally, CCL2 decoy inhibitor diminished tumor cell transmigration through endothelium in the presence of monocytes *in vitro*, which is in agreement with previous data [13,14]. These findings indicate that targeting CCL2-induced vascular activation is likely the mechanism of dnCCL2-HSA chimera in reducing metastasis.

Inhibition of the CCL2-CCR2 chemokine axis in various animal models provided a strong evidence for effective control of both primary

tumor and metastasis [12,13,33]. However, CCL2 appears to modulate monocyte activity depending on a cellular context. In a breast cancer model, CCL2 had a protumorigenic activity at the primary site, whereas it inhibited lung metastasis [35]. Recent findings showed that surgical manipulation enhances the metastatic burden by increasing tumor cell binding to the lung and liver vasculature and as a consequence causes an increased metastatic colonization of these organs [36]. Therefore, understanding the inhibitory mechanism of the CCL2-CCR2 axis is critical for evaluating this strategy for a clinical application. Especially the involvement of GAGs has so far been underestimated, and its mechanisms *in vivo* have remained elusive.

The mechanism of the dnCCL2-HSA chimera action appears to be different to CCL2-neutralizing antibodies [12,13]. Here, we show that dnCCL2-HSA chimera efficiently accumulates around the metastatic tumors cell in the lungs. We also could not observe altered leukocyte numbers in peripheral blood upon dnCCL2-HSA chimera treatment. On the contrary, systemic use of CCR2 inhibitor significantly reduced also the levels of circulating inflammatory monocytes due to its activity at the bone marrow, where the egress of monocytes has been affected [33]. Hence, the dnCCL2-HSA chimera treatment is likely influencing the local metastatic microenvironment in the target tissue (lungs) but does not affect monocyte egress from the bone marrow.

Tumor cell–activated endothelium induced local expression of SDC4, which timely correlated with an increased presence of dnCCL2-HSA chimera around the tumor cells. Whether proteoglycan families other than syndecans and glypicans are involved remains to be determined. Previously, in a mouse model of inflammation, a specific upregulation of SDC4 in the lungs has been detected [37]. Further analysis showed that TNF-α stimulation of endothelial cells upregulates SDC4 expression [38]. GAG binding and oligomerization of chemokines are essential for their activity *in vivo* [18]. Furthermore, syndecans (1 and 4) on macrophages were shown to bind to chemokines such as CCL5, and the enzymatic removal of GAGs significantly reduced chemokine activity [39]. Rationally designed CCL2 decoy protein with enhanced GAG binding activity and with CCR2-antagonist activity showed a potent anti-inflammatory activity *in vivo* [21]. The further development of the CCL2 decoy protein, dnCCL2-HSA chimera (named as GAGbodyTM), reveals also a potent inhibitory activity of CCL2-mediated tumor cell trans-endothelial migration and tumor cell extravasation. We show that the dnCCL2-HSA chimera efficiently localizes to the tumor cell–activated vasculature *in vivo*. Thus, the CCL2 decoy strategy using dnCCL2-HSA chimera represents an attractive alternative for targeting chemokines in a defined microenvironment during metastasis.

Acknowledgements

We thank Ruth Hillemann and Daniel Kull from the Institute of Virology, Technical University Munichm, and Helmholz-Zentrum Munchen for preparing slides and immunohistochemical stainings. This work was supported by a grant from EuroNanoMed2 project NANODIATER managed by the Swiss National Foundation #31NM30-136033 (L.B.) and ERC starting grant LiverCancerMechanism (M.H.).

References

[1] Balkwill F (2004). Cancer and the chemokine network. *Nat Rev Cancer* **4**, 540–550.
[2] Allavena P, Germano G, Marchesi F, and Mantovani A (2011). Chemokines in cancer related inflammation. *Exp Cell Res* **317**, 664–673.
[3] Borsig L, Wolf MJ, Roblek M, Lorentzen A, and Heikenwalder M (2014). Inflammatory chemokines and metastasis—tracing the accessory. *Oncogene* **33**, 3217–3224.
[4] Salcedo R, Ponce ML, Young HA, Wasserman K, Ward JM, Kleinman HK, Oppenheim JJ, and Murphy WJ (2000). Human endothelial cells express CCR2 and respond to MCP-1: direct role of MCP-1 in angiogenesis and tumor progression. *Blood* **96**, 34–40.
[5] Fridlender ZG, Kapoor V, Buchlis G, Cheng G, Sun J, Wang LC, Singhal S, Snyder LA, and Albelda SM (2011). Monocyte chemoattractant protein-1 blockade inhibits lung cancer tumor growth by altering macrophage phenotype and activating CD8+ cells. *Am J Respir Cell Mol Biol* **44**, 230–237.
[6] Lesokhin AM, Hohl TM, Kitano S, Cortez C, Hirschhorn-Cymerman D, Avogadri F, Rizzuto GA, Lazarus JJ, Pamer EG, and Houghton AN, et al (2012). Monocytic CCR2(+) myeloid-derived suppressor cells promote immune escape by limiting activated CD8 T-cell infiltration into the tumor microenvironment. *Cancer Res* **72**, 876–886.
[7] Fang WB, Jokar I, Zou A, Lambert D, Dendukuri P, and Cheng N (2012). CCL2/CCR2 chemokine signaling coordinates survival and motility of breast cancer cells through Smad3 protein- and p42/44 mitogen-activated protein kinase (MAPK)–dependent mechanisms. *J Biol Chem* **287**, 36593–36608.
[8] Said N, Sanchez-Carbayo M, Smith SC, and Theodorescu D (2012). RhoGDI2 suppresses lung metastasis in mice by reducing tumor versican expression and macrophage infiltration. *J Clin Invest* **122**, 1503–1518.
[9] Chiu HY, Sun KH, Chen SY, Wang HH, Lee MY, Tsou YC, Jwo SC, Sun GH, and Tang SJ (2012). Autocrine CCL2 promotes cell migration and invasion via PKC activation and tyrosine phosphorylation of paxillin in bladder cancer cells. *Cytokine* **59**, 423–432.
[10] Roca H, Varsos Z, and Pienta KJ (2008). CCL2 protects prostate cancer PC3 cells from autophagic death via phosphatidylinositol 3-kinase/AKT-dependent survivin up-regulation. *J Biol Chem* **283**, 25057–25073.
[11] Zhang J, Patel L, and Pienta KJ (2010). CC chemokine ligand 2 (CCL2) promotes prostate cancer tumorigenesis and metastasis. *Cytokine Growth Factor Rev* **21**, 41–48.
[12] Lu X and Kang Y (2009). Chemokine (C-C motif) ligand 2 engages CCR2+ stromal cells of monocytic origin to promote breast cancer metastasis to lung and bone. *J Biol Chem* **284**, 29087–29096.
[13] Qian BZ, Li J, Zhang H, Kitamura T, Zhang J, Campion LR, Kaiser EA, Snyder LA, and Pollard JW (2011). CCL2 recruits inflammatory monocytes to facilitate breast-tumour metastasis. *Nature* **475**, 222–225.
[14] Wolf MJ, Hoos A, Bauer J, Boettcher S, Knust M, Weber A, Simonavicius N, Schneider C, Lang M, and Sturzl M, et al (2012). Endothelial CCR2 signaling induced by colon carcinoma cells enables extravasation via the JAK2-Stat5 and p38MAPK pathway. *Cancer Cell* **22**, 91–105.
[15] Zhao L, Lim SY, Gordon-Weeks AN, Tapmeier TT, Im JH, Cao Y, Beech J, Allen D, Smart S, and Muschel RJ (2013). Recruitment of a myeloid cell subset (CD11b/Gr1(mid))via CCL2/CCR2 promotes thedevelopment of colorectal cancer liver metastasis. *Hepatology* **57**, 829–839.
[16] Hiratsuka S, Ishibashi S, Tomita T, Watanabe A, Akashi-Takamura S, Murakami M, Kijima H, Miyake K, Aburatani H, and Maru Y (2013). Primary tumours modulate innate immune signalling to create pre-metastatic vascular hyperpermeability foci. *Nat Commun* **4**, 1853.
[17] Adage T, Piccinini AM, Falsone A, Trinker M, Robinson J, Gesslbauer B, and Kungl AJ (2012). Structure-based design of decoy chemokines as a way to explore the pharmacological potential of glycosaminoglycans. *Br J Pharmacol* **167**, 1195–1205.
[18] Proudfoot AE, Handel TM, Johnson Z, Lau EK, LiWang P, Clark-Lewis I, Borlat F, Wells TN, and Kosco-Vilbois MH (2003). Glycosaminoglycan binding and oligomerization are essential for the in vivo activity of certain chemokines. *Proc Natl Acad Sci U S A* **100**, 1885–1890.
[19] Proudfoot AE, Power CA, Hoogewerf AJ, Montjovent MO, Borlat F, Offord RE, and Wells TN (1996). Extension of recombinant human RANTES by the retention of the initiating methionine produces a potent antagonist. *J Biol Chem* **271**, 2599–2603.
[20] Liehn EA, Piccinini AM, Koenen RR, Soehnlein O, Adage T, Fatu R, Curaj A, Popescu A, Zernecke A, and Kungl AJ, et al (2010). A new monocyte chemotactic protein-1/chemokine CC motif ligand-2 competitor limiting neointima formation and myocardial ischemia/reperfusion injury in mice. *J Am Coll Cardiol* **56**, 1847–1857.
[21] Piccinini AM, Knebl K, Rek A, Wildner G, Diedrichs-Mohring M, and Kungl AJ (2010). Rationally evolving MCP-1/CCL2 into a decoy protein with potent anti-inflammatory activity in vivo. *J Biol Chem* **285**, 8782–8792.
[22] Gerlza T, Winkler S, Atlic A, Zankl C, Konya V, Kitic N, Strutzmann E, Knebl K, Adage T, and Heinemann A, et al (2015). Designing a mutant CCL2-HSA chimera with high glycosaminoglycan-binding affinity and selectivity. *Protein Eng Des Sel* **28**, 231–240.

[23] Hoos A, Protsyuk D, and Borsig L (2014). Metastatic growth progression caused by PSGL-1-mediated recruitment of monocytes to metastatic sites. *Cancer Res* **74**, 695–704.

[24] Borsig L, Wong R, Hynes RO, Varki NM, and Varki A (2002). Synergistic effects of L- and P-selectin in facilitating tumor metastasis can involve non-mucin ligands and implicate leukocytes as enhancers of metastasis. *Proc Natl Acad Sci U S A* **99**, 2193–2198.

[25] Gerlza T, Hecher B, Jeremic D, Fuchs T, Gschwandtner M, Falsone A, Gesslbauer B, and Kungl AJ (2014). A combinatorial approach to biophysically characterise chemokine-glycan binding affinities for drug development. *Molecules* **19**, 10618–10634.

[26] Läubli H and Borsig L (2010). Selectins as mediators of lung metastasis. *Cancer Microenviron* **3**, 97–105.

[27] Stamatovic SM, Keep RF, Kunkel SL, and Andjelkovic AV (2003). Potential role of MCP-1 in endothelial cell tight junction 'opening': signaling via Rho and Rho kinase. *J Cell Sci* **116**, 4615–4628.

[28] Dzenko KA, Song L, Ge S, Kuziel WA, and Pachter JS (2005). CCR2 expression by brain microvascular endothelial cells is critical for macrophage transendothelial migration in response to CCL2. *Microvasc Res* **70**, 53–64.

[29] Serbina NV and Pamer EG (2006). Monocyte emigration from bone marrow during bacterial infection requires signals mediated by chemokine receptor CCR2. *Nat Immunol* **7**, 311–317.

[30] Soehnlein O, Drechsler M, Doring Y, Lievens D, Hartwig H, Kemmerich K, Ortega-Gomez A, Mandl M, Vijayan S, and Projahn D, et al (2013). Distinct functions of chemokine receptor axes in the atherogenic mobilization and recruitment of classical monocytes. *EMBO Mol Med* **5**, 471–481.

[31] Lebre MC, Vergunst CE, Choi IY, Aarrass S, Oliveira AS, Wyant T, Horuk R, Reedquist KA, and Tak PP (2011). Why CCR2 and CCR5 blockade failed and why CCR1 blockade might still be effective in the treatment of rheumatoid arthritis. *PLoS One* **6**, e21772.

[32] Loberg RD, Ying C, Craig M, Day LL, Sargent E, Neeley C, Wojno K, Snyder LA, Yan L, and Pienta KJ (2007). Targeting CCL2 with systemic delivery of neutralizing antibodies induces prostate cancer tumor regression in vivo. *Cancer Res* **67**, 9417–9424.

[33] Sanford DE, Belt BA, Panni RZ, Mayer A, Deshpande AD, Carpenter D, Mitchem JB, Plambeck-Suess SM, Worley LA, and Goetz BD, et al (2013). Inflammatory monocyte mobilization decreases patient survival in pancreatic cancer: a role for targeting the CCL2/CCR2 axis. *Clin Cancer Res* **19**, 3404–3415.

[34] Seetharam S, Puchalski TA, McIntosh T, Chaturvedi S, Dawkins F, Elsayed Y, Tolcher AW, Pienta KJ, de Bono JS, and C.H. T (2011). Development of biologics targeting soluble ligands: novel biomarker and PK-PD analyzes examining free and total ligand profile following treatment with carlumab (anti-CCL2 mAb). *Mol Cancer Ther* **10**, A37.

[35] Granot Z, Henke E, Comen EA, King TA, Norton L, and Benezra R (2011). Tumor entrained neutrophils inhibit seeding in the premetastatic lung. *Cancer Cell* **20**, 300–314.

[36] Cools-Lartigue J, Spicer J, McDonald B, Gowing S, Chow S, Giannias B, Bourdeau F, Kubes P, and Ferri L (2013). Neutrophil extracellular traps sequester circulating tumor cells and promote metastasis. *J Clin Invest* **123**, 3446–3458.

[37] Tanino Y, Chang MY, Wang X, Gill SE, Skerrett S, McGuire JK, Sato S, Nikaido T, Kojima T, and Munakata M, et al (2012). Syndecan-4 regulates early neutrophil migration and pulmonary inflammation in response to lipopolysaccharide. *Am J Respir Cell Mol Biol* **47**, 196–202.

[38] Okuyama E, Suzuki A, Murata M, Ando Y, Kato I, Takagi Y, Takagi A, Murate T, Saito H, and Kojima T (2013). Molecular mechanisms of syndecan-4 upregulation by TNF-alpha in the endothelium-like EAhy926 cells. *J Biochem* **154**, 41–50.

[39] Charni F, Friand V, Haddad O, Hlawaty H, Martin L, Vassy R, Oudar O, Gattegno L, Charnaux N, and Sutton A (2009). Syndecan-1 and syndecan-4 are involved in RANTES/CCL5-induced migration and invasion of human hepatoma cells. *Biochim Biophys Acta* **1790**, 1314–1326.